

# 13

## Combined Plastic Bending and Compression or Tension

### 13.1 GENERALIZED PLASTIC HINGE

So far we have assumed that a plastic hinge forms if the bending moment in a critical cross section reaches the plastic limit value,  $M_0$ . We have tacitly neglected the effect of the other internal forces on the formation of the yield hinge. This effect, however, can be appreciable, for example in multi-storey frames or frames with a large horizontal thrust where the axial forces are large. So, we will now refine our analysis and consider the interaction of bending moment  $M$  and normal force  $N$ . The resulting fully plasticized cross section will be referred to as a *generalized plastic hinge*. The effect of the shear force is usually less important, and is also more difficult to incorporate. We will postpone this problem to Part III, because it is beyond the scope of analysis under uniaxial stress.

A typical evolution of the strain and stress profiles during the formation of a generalized plastic hinge is depicted in Figure 13.1. As usual, it may be assumed that the cross sections remain planar at all stages of the loading process. Consequently, the variation of normal strains over the cross section is linear. The corresponding stress distribution is linear only in the elastic range (Figure 13.1(a)). As the loading process continues, yielding starts at the top or bottom fibers, and the plastic zone propagates into the interior of the cross section (Figure 13.1(b)). During the elastoplastic stage, the cross section has an elastic core with linear stress variation, and one or two plastic zones with constant stress equal to the positive or negative yield stress. For very large curvatures, the elastic core becomes negligibly small, and the stress distribution approaches a piecewise constant distribution, with one part of the cross section yielding in tension and the remaining part yielding in compression.

The plasticization process of course takes place in the neighboring cross sections as well, and the plastic zone occupies a certain volume (Figure 13.2(b)). However, for the purpose of modeling, we can lump the plastic hinge into one single cross section, the same as we did while analyzing the hinge under pure bending. The total plastic deformation in the idealized hinge is replaced by a rotation,  $\theta$ , and longitudinal displacement,  $e_p$  (Figure 13.2(c)). From kinematic considerations, it follows that the plastic extension at an arbitrary point of the plasticized cross section can be expressed by a linear function

$$\bar{e}_p(z) = e_p + \theta z \quad (13.1)$$

where  $z$  is the centroidal coordinate perpendicular to the bending axis. The plastic extension at the centroid,  $\bar{e}_p(0) = e_p$ , corresponds to the 'gap' between the centroids

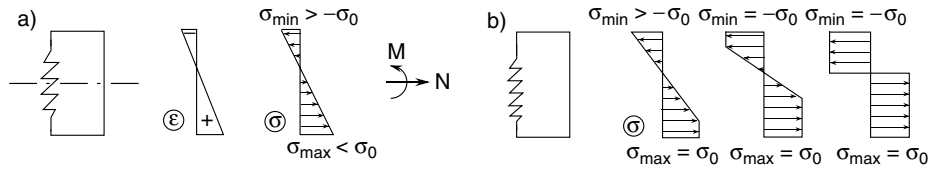


Figure 13.1 Strain and stress distributions

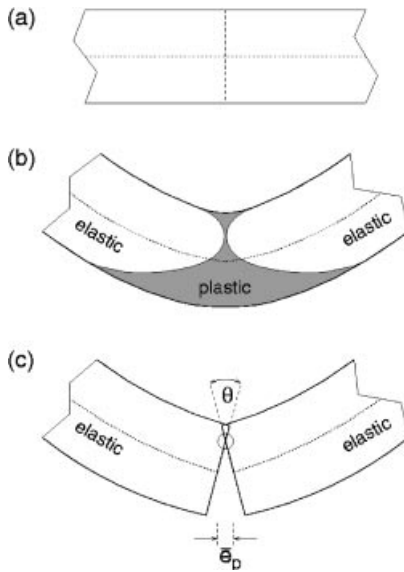


Figure 13.2 Generalized plastic hinge

of the end cross sections of the two elastic parts connected by the generalized yield hinge in Figure 13.2(c). The bar over  $e$  helps to distinguish the distribution of the plastic extension over the cross section,  $\bar{e}_p(z)$ , which is a function of the distance from the centroidal axis, from the variable  $e_p$ , which characterizes the deformation of the generalized plastic hinge and is equal to the value of  $\bar{e}_p$  at  $z = 0$ .

Consider a given distribution of plastic extension, represented by the solid line in Figure 13.3(a). It might seem natural to assume that the fibers for which  $\bar{e}_p(z) > 0$  yield in tension, and those for which  $\bar{e}_p(z) < 0$  yield in compression; see Figure 13.4(b). This assumption corresponds to the so-called *deformation theory of plasticity*, in which

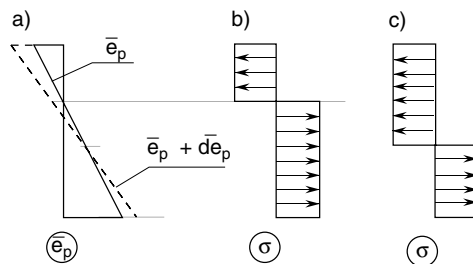


Figure 13.3 Distribution of a) strain, b) stress according to the deformation theory, c) stress according to the flow theory of plasticity

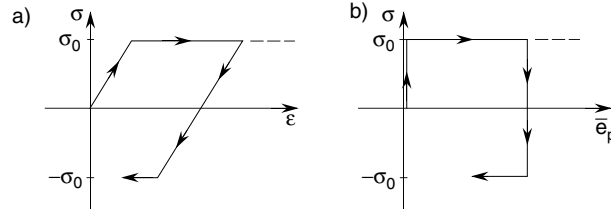


Figure 13.4 Stress-strain and stress-extension diagrams

the stress state is entirely determined by the current strain state, independently of the previous history of strain evolution (Hencky, 1924). Such a model is conceptually simple and convenient, but not always sufficiently realistic. The actual stress in an elastoplastic material is uniquely determined by the strain only as long as the loading process is monotonic. If the strain increment changes its sign, the material unloads elastically and eventually starts yielding in the opposite direction (Figure 13.4(a)). The deformation of a plastic hinge does not have any elastic component, and so the stress jumps to the opposite yield stress immediately after the plastic extension increment has changed its sign (Figure 13.4(b)). Clearly, the stress can be negative even at a positive extension. If we strictly adhere to the *flow theory of plasticity* we have to determine the sign of stress from the sign of plastic extension rate (increment) rather than from the sign of the plastic extension itself. This means that the position of the neutral axis separating the tensile zone from the compressive zone is determined by the condition  $\dot{\bar{\epsilon}}_p(z) = 0$  rather than  $\bar{\epsilon}_p(z) = 0$ ; see Figure 13.3(c).

Depending on the position of the neutral axis, a generalized plastic hinge can yield different combinations of internal forces  $M$  and  $N$ . The set of all such combinations is the so-called *plastic limit envelope* in the space of internal forces (also called the yield surface, yield locus, failure envelope, or interaction curve). States outside this envelope can never be reached. Similarly to the plastic hinge under pure bending, it is assumed that states inside the plastic limit envelope are entirely elastic, although this is not exactly true. One could define the *elastic limit envelope* that corresponds to states at which the first point of a cross section begins yielding (similar to the limit elastic moment in the case of pure bending). The states between the elastic and plastic limit envelopes are elastoplastic, but the corresponding plastic deformations that precede the formation of a full plastic hinge are usually neglected, especially when looking for the final collapse mechanism rather than for the details of the response in the elastoplastic range.

**Example 13.1:** Construct the elastic limit envelope and the plastic limit envelope for a rectangular cross section of width  $b$  and depth  $h$ .

**Solution:** 1) We start with the plastic limit envelope. Let us specify the position of the neutral axis by the coordinate  $z_n = \eta h/2$  measured from the cross section centroid (Figure 13.5). Instead of integrating over the cross section, we can replace the positive stress by its resultant

$$N^+ = A^+ \sigma_0 = \frac{1}{2}(1 - \eta)bh\sigma_0 \quad (13.2)$$

and the negative stress by its resultant

$$N^- = A^- \sigma_0 = \frac{1}{2}(1 + \eta)bh\sigma_0 \quad (13.3)$$

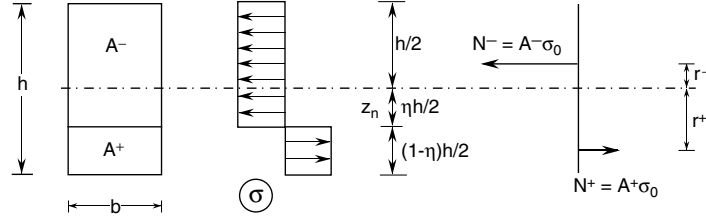


**Figure 13.5** Stress distributions in a rectangular cross section

as indicated in Figure 13.5. The arms of the resultants of positive and negative stress, i.e. the distances of the centroids of the areas under tension and under compression from the centroid of the entire cross section, are given by

$$r^+ = \frac{\eta h}{2} + \frac{1}{2}(1-\eta)\frac{h}{2} = \frac{1}{4}(1+\eta)h \quad (13.4)$$

$$r^- = \frac{1}{2}(1+\eta)\frac{h}{2} - \frac{\eta h}{2} = \frac{1}{4}(1-\eta)h \quad (13.5)$$

The force and moment resultants at a plastic limit state are now obtained as

$$N = \int_A \sigma \, dA = N^+ - N^- = -\sigma_0 b h \eta \quad (13.6)$$

$$\begin{aligned} M &= \int_A \sigma z \, dA = N^+ r^+ + N^- r^- \\ &= \frac{1}{2}(1-\eta) b h \sigma_0 \times \frac{1}{4}(1+\eta)h + \frac{1}{2}(1+\eta) b h \sigma_0 \times \frac{1}{4}(1-\eta)h \\ &= \frac{1}{4} \sigma_0 b h^2 (1-\eta^2) \end{aligned} \quad (13.7)$$

The parameter  $\eta$  describing the position of the neutral axis can vary within the limits  $[-1, 1]$ . The values  $\eta = -1$ ,  $\eta = 0$  and  $\eta = 1$  correspond to the axial tension, pure bending and axial compression, respectively. For  $\eta = -1$ , the normal force assumes its maximum possible value,  $N = \sigma_0 b h \equiv N_0 =$  plastic normal force, while the bending moment is zero. For  $\eta = 0$ , the bending moment assumes its maximum possible value,  $M = \sigma_0 b h^2 / 4 \equiv M_0 =$  plastic moment, while the normal force is zero. Finally, for  $\eta = 1$ , the normal force assumes its minimum possible value,  $N = -\sigma_0 b h = -N_0$ , while the bending moment is zero. Note that the plastic normal force  $N_0$  is identical to the plastic axial force  $S_0$  we introduced in truss analysis; likewise,  $N$  and  $S$  are only two alternative symbols for the normal, or axial, force.

Relations (13.6) and (13.7), rewritten as

$$\left. \begin{aligned} N &= -N_0 \eta \\ M &= M_0 (1 - \eta^2) \end{aligned} \right\} -1 \leq \eta \leq 1 \quad (13.8)$$

parametrically describe the plastic limit envelope. Eliminating the parameter  $\eta$ , we get an explicit equation for the envelope,

$$\frac{M}{M_0} = 1 - \left( \frac{N}{N_0} \right)^2, \quad -1 \leq \frac{N}{N_0} \leq 1 \quad (13.9)$$

which obviously defines a parabolic arc.

Deriving the previous results, we have tacitly assumed that the bottom face of cross section is under tension and the top face under compression. In other words, equation (13.9) only applies if the bending moment is positive. To obtain a complete description of the plastic limit envelope, we have to consider the opposite case of tension at the top face and compression at the bottom. Reverting the signs of stresses and, consequently, of the internal forces, we get

$$\left. \begin{aligned} N &= N_0\eta \\ M &= -M_0(1 - \eta^2) \end{aligned} \right\} -1 \leq \eta \leq 1 \quad (13.10)$$

from which

$$\frac{M}{M_0} = -1 + \left(\frac{N}{N_0}\right)^2, \quad -1 \leq \frac{N}{N_0} \leq 1 \quad (13.11)$$

This equation describes a parabolic arc that is a mirror image of the previous one. The complete plastic limit envelope is shown as the solid curve in Figure 13.6.

Relations (13.9) and (13.11), separately describing the upper and lower branches of the plastic limit envelope, can be replaced by a single equation

$$f(N, M) \equiv \left(\frac{N}{N_0}\right)^2 + \left|\frac{M}{M_0}\right| - 1 = 0 \quad (13.12)$$

Note that the interior of the plastic limit envelope is characterized by  $f(N, M) < 0$ , and its exterior by  $f(N, M) > 0$ . A function  $f$  with this property is called the *yield function*.

2) The elastic limit envelope can easily be determined using the well-known expressions for stresses in the extreme points of the cross section,

$$\sigma_{max} = \frac{N}{A} + \frac{M}{W_{el}} \quad (13.13)$$

$$\sigma_{min} = \frac{N}{A} - \frac{M}{W_{el}} \quad (13.14)$$

where  $A = bh$  is the cross sectional area, and  $W_{el} = bh^2/6$  is the elastic cross sectional modulus. The section remains elastic as long as  $|\sigma| \leq \sigma_0$ , i.e. the values of internal forces in the elastic domain satisfy the condition

$$\left| \frac{N}{\sigma_0 A} \pm \frac{M}{\sigma_0 W_{el}} \right| \leq 1 \quad (13.15)$$

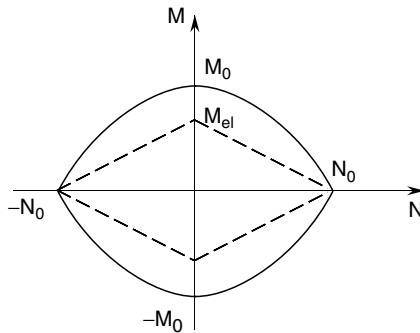


**Figure 13.6** Elastic and plastic limit envelopes for a rectangular cross section

Note that (13.15) represents four inequalities that must be satisfied simultaneously. Using the relations  $\sigma_0 A = N_0$  and  $\sigma_0 W_{el} = M_{el}$  we can rewrite the condition as

$$\left| \frac{N}{N_0} \pm \frac{M}{M_{el}} \right| \leq 1 \quad (13.16)$$

The previous description of the elastic domain applies to cross sections of an arbitrary shape, not only to rectangular ones. According to (13.16), the elastic domain is a parallelogram whose vertices correspond to the elastic limits under axial tension or compression, and under pure bending. Under axial tension or compression, the elastic limit coincides with the plastic limit. Under pure bending, the ratio  $M_0/M_{el} = \alpha$  depends on the shape of the cross section. For rectangular cross sections,  $\alpha = 1.5$ , and the corresponding elastic limit envelope is marked in Figure 13.6 by the dashed lines.  $\square$

Let us now explore the relation between the plastic deformations and the changes of internal forces. A generalized plastic hinge forms at a certain cross section when the internal forces reach the plastic limit envelope. In contrast to the plastic hinge under pure bending, the values of the internal forces do not have to remain constant as the hinge deforms. During plastic flow, the neutral axis can change its location while the cross section remains entirely plasticized. Consequently, the internal forces transmitted by the hinge move along the plastic limit envelope.

As explained before, the location of the neutral axis is determined, according to the deformation theory of plasticity, by the current values of the generalized strains  $e$  and  $\theta$  or, according to the flow theory of plasticity, by their rates  $\dot{e}$  and  $\dot{\theta}$ . The neutral axis divides the cross section into the part yielding in tension,  $A^+$ , and the part yielding in compression,  $A^-$ ; see Figure 13.7. For a general cross section, the internal forces can be expressed as

$$N = \int_{A^+} \sigma_0 dA + \int_{A^-} (-\sigma_0) dA = \sigma_0(A^+ - A^-) \quad (13.17)$$

$$M = \int_{A^+} \sigma_0 z dA + \int_{A^-} (-\sigma_0) z dA = \sigma_0(S^+ - S^-) \quad (13.18)$$

where

$$S^+ = \int_{A^+} z dA \quad (13.19)$$

is the static moment of the part under tension with respect to the centroidal axis, and

$$S^- = \int_{A^-} z dA \quad (13.20)$$

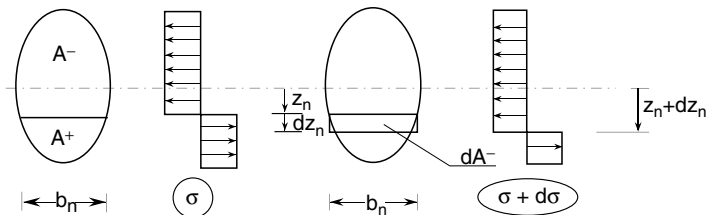


Figure 13.7 Change of neutral axis

is the static moment of the part under compression. Let  $z_n$  denote the current position of the neutral axis. If the neutral axis currently located at  $z_n$  moves by an infinitesimal distance  $dz_n$ , the corresponding increments of the areas and static moments can be expressed as

$$dA^+ = -b_n dz_n \tag{13.21}$$

$$dA^- = b_n dz_n \tag{13.22}$$

$$dS^+ = z_n dA^+ = -b_n z_n dz_n \tag{13.23}$$

$$dS^- = z_n dA^- = b_n z_n dz_n \tag{13.24}$$

where  $b_n$  is the width of the cross section at the current level of the neutral axis; see Figure 13.7. Consequently, the internal forces change by

$$dN = \sigma_0(dA^+ - dA^-) = -2\sigma_0 b_n dz_n \tag{13.25}$$

$$dM = \sigma_0(dS^+ - dS^-) = -2\sigma_0 b_n z_n dz_n = z_n dN \tag{13.26}$$

The fact that the slope of the plastic limit envelope is equal to the distance of the neutral axis from the centroid, i.e.

$$\frac{dM}{dN} = z_n \tag{13.27}$$

has very important implications:

1. **Convexity:** As the position of the neutral axis changes from the bottom of the cross section ( $z_n = z_{max} > 0$ ) to the top ( $z_n = z_{min} < 0$ ), the corresponding point on the plastic limit envelope travels along the upper branch from the left corner to the right corner, and along the lower branch from the right to the left; see Figure 13.8. During this process, the slope  $dM/dN = z_n$  monotonically decreases. Consequently, for the upper branch we have  $d^2M/dN^2 < 0$ , and for the lower branch  $d^2M/dN^2 > 0$ . This implies that the interior of the plastic limit envelope is a *convex domain*.

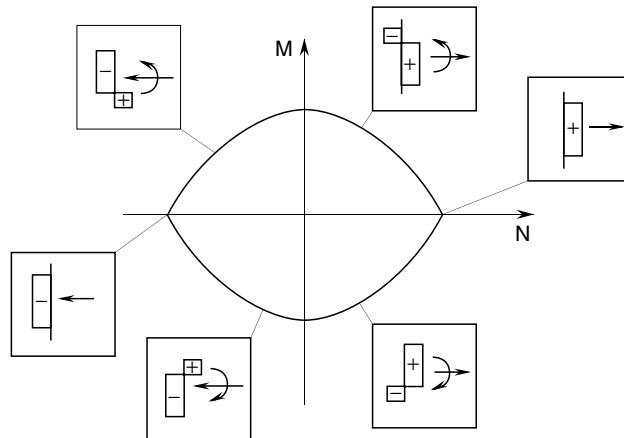


Figure 13.8 Plastic limit envelope with stress distributions

2. **Normality:** Recall that, according to the flow theory of plasticity, the position of the neutral axis is determined by the condition

$$\dot{e}_p(z_n) \equiv \dot{e}_p + \dot{\theta}z_n = 0 \quad (13.28)$$

Combining this with the rate form of (13.27),

$$\frac{\dot{M}}{\dot{N}} = z_n \quad (13.29)$$

we obtain

$$\dot{N}\dot{e}_p + \dot{M}\dot{\theta} = 0 \quad (13.30)$$

or

$$\dot{\mathbf{s}}^T \dot{\mathbf{e}}_p = 0 \quad (13.31)$$

where

$$\mathbf{s} = \left\{ \begin{array}{c} N \\ M \end{array} \right\} \quad (13.32)$$

is the vector of internal forces and

$$\mathbf{e}_p = \left\{ \begin{array}{c} e_p \\ \theta \end{array} \right\} \quad (13.33)$$

is the vector of plastic generalized strains that is work-conjugate to  $\mathbf{s}$ .

During plastic flow, full plasticity of the cross section is preserved. Consequently, vector  $\mathbf{s}$  travels along the yield surface (plastic limit envelope), and so vector  $\dot{\mathbf{s}}$  represents the direction of the tangent to the yield surface; see Figure 13.9. Now we plot the plastic deformations in the same figure; we superimpose the axial extension  $e_p$  on axis  $N$ , and rotation  $\theta$  on axis  $M$ . The plastic deformation rate vector,  $\dot{\mathbf{e}}_p$ , may now be displayed in the plane of internal forces. Equation (13.31) means that the scalar product of the tangent vector  $\dot{\mathbf{s}}$  and the plastic deformation rate vector  $\dot{\mathbf{e}}_p$  is zero, and so these vectors are orthogonal.<sup>1</sup>

We have thus deduced a very important property, which is typical not just for the interaction of normal force and bending moment, but for many types of plastic behavior, in general called *associated plasticity*.

**Normality rule:** *The increment of the plastic deformation vector has the direction of the normal to the yield surface (plastic limit envelope) at the point representing the current internal forces.*

At the corner points  $A$  and  $E$  in Figure 13.9, the preceding conclusion is ambiguous and does not apply literally. For those points the stress is uniformly distributed and equal to  $\sigma_0$  or  $-\sigma_0$ . Such a uniform stress distribution occurs not only for pure extension ( $\dot{\theta} = 0$ ), but also for all rotation rates for which the neutral axis location  $z_n = -\dot{e}_p/\dot{\theta}$  lies outside the interval  $(z_{min}, z_{max})$ . All such  $z_n$  locations

---

<sup>1</sup> Strictly speaking, the vectors are orthogonal in the standard geometric sense only if the scales on the axes are chosen such that the 'work product'  $\dot{\mathbf{s}}^T \dot{\mathbf{e}}_p$  be identical with the standard scalar product of geometric vectors.

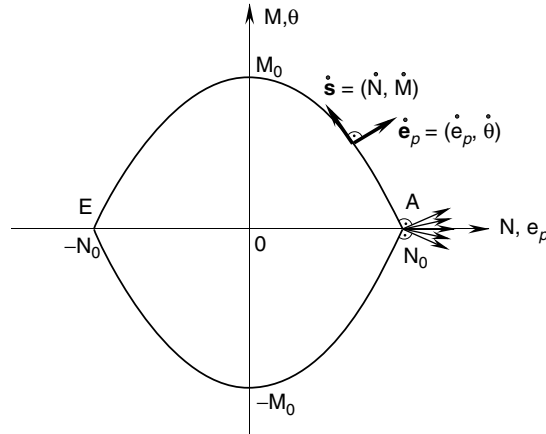


Figure 13.9 Normality rule

represent the case of uniform tension, or of uniform compression, depending on the sign of  $\dot{e}_p$ . A uniform stress distribution is obtained for any  $z_n$  between  $z_{max}$  and  $\infty$ , or between  $-\infty$  and  $z_{min}$ . For the limit cases  $z_n = z_{max}$  and  $z_n = z_{min}$  the preceding derivation applies, and so the vector  $\dot{e}_p$  is normal to the upper branch of the yield surface at point A (if  $\dot{\theta} = -\dot{e}_p/z_{min} > 0$ ), or to its lower branch (if  $\dot{\theta} = -\dot{e}_p/z_{max} < 0$ ); see Figure 13.9. For any intermediate value of  $\dot{\theta}$ , the plastic deformation rate vector  $\dot{e}$  lies between the directions for the two limiting cases. Thus, we reach the following important conclusion for a corner on the yield surface (also known as a *vertex*).

**Normality rule at a corner:** *The increment of the plastic deformation vector at a corner of the yield surface lies within a fan of directions limited by the normals to the yield surface on both sides of the corner.*

This rule has a broad validity, not limited to the interaction of normal forces and bending moments. In the deformation theory of plasticity, similar statements hold when we replace the increments of plastic generalized strains by their total values.

### 13.2 BASIC THEOREMS

Recall that the dissipation power (under uniaxial stress) is defined as

$$D_{\text{int}} = \int_V \sigma \dot{\epsilon}_p \, dV \tag{13.34}$$

where  $\dot{\epsilon}_p$  is the plastic strain rate. Plastic strains in a generalized plastic hinge are lumped into the plastic extensions  $\bar{e}_p(z)$  that are concentrated in a single cross section. Consequently, the rate of dissipation in a single hinge can be expressed as

$$D_{\text{int}} = \int_A \sigma(z) \dot{\bar{e}}_p(z) \, dA \tag{13.35}$$

because the extension  $\bar{e}_p(z)$  corresponds to the plastic strain integrated over the length of the plastic hinge. Substituting expression (13.1) for the plastic extension, we can

transform (13.35) into

$$D_{\text{int}} = \int_A \sigma(z)(\dot{e}_p + \dot{\theta}z) dA = \int_A \sigma(z) dA \dot{e}_p + \int_A \sigma(z) z dA \dot{\theta} = N\dot{e}_p + M\dot{\theta} \quad (13.36)$$

The dissipative work is done by the normal force on the plastic extension of the beam axis, and by the bending moment on the rotation of the plastic hinge. Setting  $N = 0$ , we obtain as a special case formula (2.22) for the dissipation power in a plastic hinge under pure bending. Setting  $M = 0$  and identifying the normal force  $N$  with the axial force  $S$ , we obtain formula (2.2) for the dissipation power in a bar under axial tension or compression. The total dissipation rate in a structure is given by the sum of dissipation rates in all plastic hinges.

The basic properties of the plastic flow in a generalized plastic hinge (convexity and normality) are closely related to the postulate of maximum plastic dissipation. In the context of multiaxial plasticity, they have to be postulated as the hypotheses of the theory; cf. Chapter 15. The actual behavior of some materials might violate these assumptions, and then a number of basic theorems that rely on the aforementioned postulate cease to hold. However, in the present context of plasticity under uniaxial stress, the postulate is almost automatic. Recall that, for one material point, we have

$$\sigma^* \dot{e}_p \leq \mathcal{D}(\dot{e}_p) \equiv \sigma \dot{e}_p \quad (13.37)$$

where  $\sigma^*$  is any plastically admissible stress,  $\dot{e}_p$  is a given plastic strain rate, and  $\mathcal{D}(\dot{e}_p)$  is the corresponding plastic dissipation rate per unit volume.

Suppose that we are given the rates of generalized strains  $\dot{e}_p$  and  $\dot{\theta}$  at a certain plastic hinge, and some values of internal forces  $N^*$  and  $M^*$  that are completely arbitrary (independent of  $\dot{e}_p$  and  $\dot{\theta}$ ), but satisfy the condition of plastic admissibility,  $f(N^*, M^*) \leq 0$ . Let us denote by  $N$  and  $M$  the actual internal forces generated by the given deformation rates, and by  $\sigma(z)$  the corresponding stress distribution. As the forces  $N^*$  and  $M^*$  are inside the plastic limit envelope, they can be represented as the resultants of a normal stress distribution  $\sigma^*(z)$  that is plastically admissible at any point of the cross section. Integrating (13.37) along each longitudinal 'fiber' of the generalized plastic hinge (i.e. along  $x$ , at constant  $y$  and  $z$ ), we have

$$\sigma^*(z) \dot{e}_p(z) \leq \sigma(z) \dot{e}_p(z) \quad (13.38)$$

Now we integrate this inequality over the entire cross section. Expressing the extension rate  $\dot{e}_p(z)$  in terms of the generalized strain rates according to (13.1) we can write the integral of the left-hand side as

$$\int_A \sigma^*(z) \dot{e}_p(z) dA = \int_A \sigma^*(z)(\dot{e}_p + \dot{\theta}z) dA = N^* \dot{e}_p + M^* \dot{\theta} = \mathbf{s}^{*T} \dot{\mathbf{e}}_p \quad (13.39)$$

and the integral of the right-hand side as

$$\int_A \sigma(z) \dot{e}_p(z) dA = \int_A \sigma(z)(\dot{e}_p + \dot{\theta}z) dA = N \dot{e}_p + M \dot{\theta} = \mathbf{s}^T \dot{\mathbf{e}}_p = D_{\text{int}}(\dot{\mathbf{e}}_p) \quad (13.40)$$

We have proven that

$$\mathbf{s}^{*T} \dot{\mathbf{e}}_p \leq D_{\text{int}}(\dot{\mathbf{e}}_p) \equiv \mathbf{s}^T \dot{\mathbf{e}}_p \quad (13.41)$$

for any plastically admissible internal forces  $\mathbf{s}^*$ . Summing the contributions of all generalized plastic hinges, we obtain a similar inequality for the entire structure. Now, vector  $\mathbf{s}$  collects the moments and normal forces at critical sections, and  $\mathbf{e}_p$  is the work-conjugate vector of plastic generalized strains.

**Postulate of maximum plastic dissipation**

*The actual internal forces  $\mathbf{s}$  corresponding to the given rates of plastic generalized strains  $\dot{\mathbf{e}}_p$  maximize the plastic dissipation rate among all the plastically admissible vectors of internal forces  $\mathbf{s}^*$ .*

The previous postulate makes it possible to extend the basic theorems of perfect elastoplasticity to frames with generalized plastic hinges. The proofs remain formally unchanged, but the internal force vector  $\mathbf{s}$  now contains both the normal forces and the bending moments, and the corresponding generalized strains  $\mathbf{e}_p$  include the plastic axial extensions and the rotations of the generalized plastic hinges. The reader is advised to review the proofs of the bound theorems of limit analysis and of the shakedown theorems in order to verify their general validity.

**Example 13.2:** Calculate the collapse load for the frame in Figure 13.10(a) taking into account the effect of axial forces. The columns and the beam have the same rectangular cross section with a depth-to-span ratio  $h/2L = 1 : 10$ .

**Solution:** We will follow the static approach. The structure is statically indeterminate to the third degree, and so we select three forces as the redundants. Our choice will be the internal forces at the cross section just to the left of the axis of symmetry, which are identical to the end forces  $X_{32}$ ,  $Z_{32}$  and  $M_{32}$ ; see Figure 13.10(b). Given the redundants plus the load  $F$ , we can calculate all the internal forces from equilibrium. If the internal forces are plastically admissible at all the critical cross sections, the state is statically admissible. Our goal is to find the statically admissible state with the largest possible value of the load  $F$ .

A simplified analysis, neglecting the effect of axial forces, leads to the beam failure mechanism that corresponds to the collapse load  $\hat{F}_0 = 4M_0/L$ . When the axial force is taken into account, we must distinguish whether the hinge in a corner of a frame forms on the column side or on the beam side of the corner. This is because the axial forces on either side of the corner are different, although the bending moment is the same. Due to the type of loading, it is reasonable to expect that the hinges form on

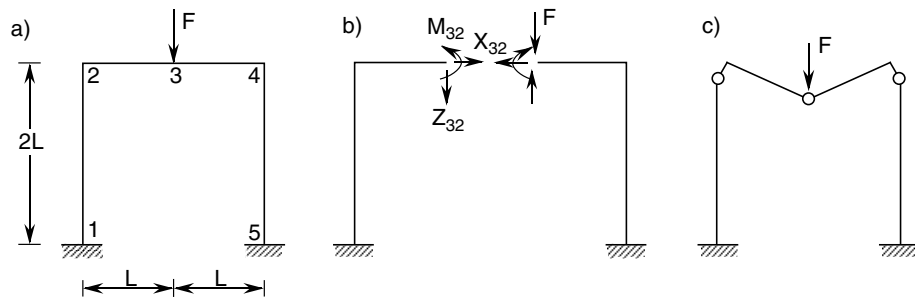


Figure 13.10 Portal frame (Example 13.2)

the column side of the corner; see Figure 13.10(c). Of course, in a complete analysis we must check the validity of this assumption once we have obtained the corresponding solution.

It immediately follows from symmetry and from equilibrium of joint 3 that  $Z_{32} = F/2$ , and so we can reduce the number of redundants to two. Based on equilibrium considerations, it is easy to compute the bending moment and normal force at cross section 21,

$$N_{21} = -\frac{1}{2}F \quad (13.42)$$

$$M_{21} = M_{32} - \frac{1}{2}FL \quad (13.43)$$

The internal forces at cross section 3 are directly the redundants  $N_{32} = X_{32}$  and  $M_{32}$ , and due to symmetry, the conditions of plastic admissibility at cross section 45 are equivalent to those at cross section 21. We are looking for a triplet  $(F, N_{32}, M_{32})$  satisfying the conditions of plastic admissibility

$$f(N_{21}, M_{21}) \leq 0 \quad \dots \quad \left(\frac{F}{2N_0}\right)^2 + \frac{|M_{32} - FL/2|}{M_0} \leq 1 \quad (13.44)$$

$$f(N_{32}, M_{32}) \leq 0 \quad \dots \quad \left(\frac{N_{32}}{N_0}\right)^2 + \frac{|M_{32}|}{M_0} \leq 1 \quad (13.45)$$

and maximizing the value of  $F$ . If the plastic normal force  $N_0$  is large compared to  $M_0/L$  we can neglect the quadratic terms in (13.44)–(13.45). The corresponding set of statically admissible solutions is graphically presented in terms of dimensionless parameters  $FL/M_0$  and  $M_{32}/M_0$  in Figure 13.11(a). The largest statically admissible load,  $\hat{F}_0 = 4M_0/L$ , is the collapse load according to the simplified analysis with axial forces neglected. When the quadratic terms are taken into account, the constraint on  $M_{32}$  dictated by (13.45) does not change, because the redundant force  $N_{32}$  does not appear in any other condition and can be set to zero (the least restrictive case). Condition (13.44) now becomes quadratic, and the corresponding straight lines are replaced by the parabolas shown in Figure 13.11(b) (where the parabolas

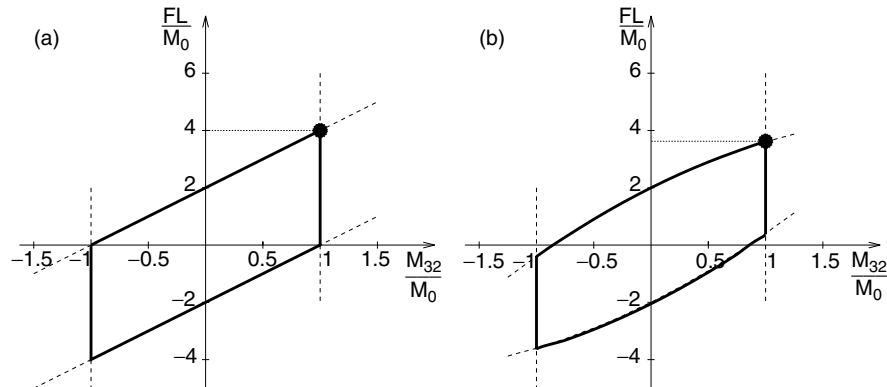


**Figure 13.11** Statically admissible domain with the effect of normal forces a) neglected, b) taken into account

are deliberately plotted for a depth-to-span ratio much higher than the prescribed one, because for  $h/2L = 1 : 10$  they would be almost identical with the straight lines from Figure 13.11(a)). For realistic depth-to-span ratios, the apex of the upper parabola is outside the interval  $-1 \leq M_{32}/M_0 \leq 1$ , and the maximum statically admissible value of  $F$  is determined by the intersection of this parabola with the straight line  $M_{32}/M_0 = 1$ . This leads to a quadratic equation for the collapse load  $F_0$ ,

$$\left(\frac{M_0}{LN_0}\right)^2 \left(\frac{F_0 L}{M_0}\right)^2 + 2\frac{F_0 L}{M_0} - 8 = 0 \quad (13.46)$$

Since  $M_0 = W_0\sigma_0 = bh^2\sigma_0/4$  and  $N_0 = A\sigma_0 = bh\sigma_0$ , the factor  $(M_0/LN_0)^2$  can be expressed as  $(h/4L)^2$ . For the given depth-to-span ratio  $h/2L = 1 : 10$  we have  $(h/4L)^2 = (1/20)^2 = 1/400$ , which means that the quadratic term in (13.46) is indeed very small compared to the linear term. The collapse load  $F_0 = 3.98M_0/L$  differs from  $\hat{F}_0$  only by 0.5%, which is negligible from the practical point of view. Even for  $h/2L = 1 : 5$  we would still get a reduction of only 2%. The simplified solution neglecting the effect of axial forces is therefore fully justified in the present situation.  $\square$

### 13.3 SIMPLE ESTIMATES OF COLLAPSE LOAD

As we have seen, an exact analysis of the collapse load of frames based on the curvilinear yield surface is possible but complicated, since it leads to nonlinear equations. This is because the limit bending moment depends nonlinearly on the limit axial force. Example 13.2 has shown that in some cases, the effect of normal forces on the collapse load is negligible, and the standard analysis taking into account only the bending moments is fully sufficient. It is therefore important to develop simple methods permitting easy detection of such situations.

The relative importance of normal forces strongly depends on the slenderness of the frame members (beams and columns). If the shape of the cross section is kept constant, the plastic limit moment grows faster than the plastic normal force when the size of the cross section increases. This means that for bulky members the effect of normal forces on the plasticization process becomes more important. It is useful to introduce the parameter

$$h_0 = \frac{M_0}{N_0} = \frac{W_0\sigma_0}{A\sigma_0} = \frac{W_0}{A} \quad (13.47)$$

which is a geometrical characteristic of the cross section and has the dimension of length. In fact,  $h_0$  is one half of the 'internal arm' in the plastic limit state, i.e. of the distance between the resultant of the tensile stresses and the resultant of the compressive stresses. For example, for a rectangular cross section we obtain

$$h_0 = \frac{W_0}{A} = \frac{bh^2/4}{bh} = \frac{h}{4} \quad (13.48)$$

The slenderness of a member is then characterized by the ratio  $\ell/h_0$  where  $\ell$  is the member length. Here we define slenderness for the purpose of plastic analysis. Note that in the analysis of elastic stability, slenderness has a different meaning – the ratio

of the effective length to the cross sectional radius of inertia; e.g. see Bažant and Cedolin (1991).

For an *ideal sandwich cross section*, which is an idealized I-section with thin flanges and a negligible web, the internal arm is equal to the full depth of the cross section,  $h$ , and so  $h_0 = h/2$ . Note also another interesting property of the ideal sandwich section: the elastic domain coincides with the elastoplastic one, i.e. the plastic limit state is reached immediately after the onset of yielding. This is related to the fact that the web is neglected and the flanges are assumed to be thin compared to the depth of the section. In particular, the plastic limit moment  $M_0$  is equal to the elastic limit moment  $M_{el}$ .

Let us denote the safety factors determined with and without taking into account the effect of normal forces by  $\mu_0$  and  $\hat{\mu}_0$ , respectively. Suppose that we have analyzed the structure by the standard technique (i.e. neglecting the effect of normal forces on the formation of plastic hinges), and we know the corresponding safety factor,  $\hat{\mu}_0$ . A rough lower bound on  $\mu_0$  can be constructed quite easily. The internal forces at collapse determined by the standard technique satisfy the equations of equilibrium but, due to the presence of nonzero normal forces, they are not plastically admissible in the generalized plastic hinges. A statically admissible state is obtained if we multiply the internal forces as well as the load multiplier by a common scalar factor such that the resulting forces become plastically admissible. This corresponds to a radial return in the space of internal forces such that the point representing the reduced state is just on the yield surface. For each critical cross section  $ij$  we determine a scaling factor  $\xi_{ij}$  from the condition

$$f(\xi_{ij}N_{ij}, \xi_{ij}M_{ij}) = 0 \quad (13.49)$$

where  $N_{ij}$  and  $M_{ij}$  are the internal forces at collapse evaluated by the standard analysis.

Multiplying the internal forces and the safety factor  $\hat{\mu}_0$  by the smallest scaling factor

$$\xi_{min} = \min_{ij} \xi_{ij} \quad (13.50)$$

we obtain a statically admissible state, and so  $\xi_{min}\hat{\mu}_0$  is a lower bound on  $\mu_0$ . If  $\xi_{min}$  is sufficiently close to 1, the effect of normal forces is negligible, and we can avoid the laborious analysis of the model with generalized plastic hinges.

**Example 13.3:** Evaluate simple bounds on the safety factor for the frame from Examples 7.3 and 7.5, reproduced in Figure 13.12(a), taking into account the effect of normal forces. Assume that the cross section is close to an ideal sandwich cross section.

**Solution:** For an ideal sandwich, the plastic limit envelope coincides with the elastic limit envelope; see Problem 13.2. From the general expression for the elastic limit envelope (13.16) and from the relation  $M_{el} = M_0$ , it follows that the condition of plastic admissibility can be written as

$$\frac{|N|}{N_0} + \frac{|M|}{M_0} \leq 1 \quad (13.51)$$

The bending moments at collapse calculated in Example 7.5 are reproduced in Figure 13.12(b), and the corresponding normal forces determined from equilibrium

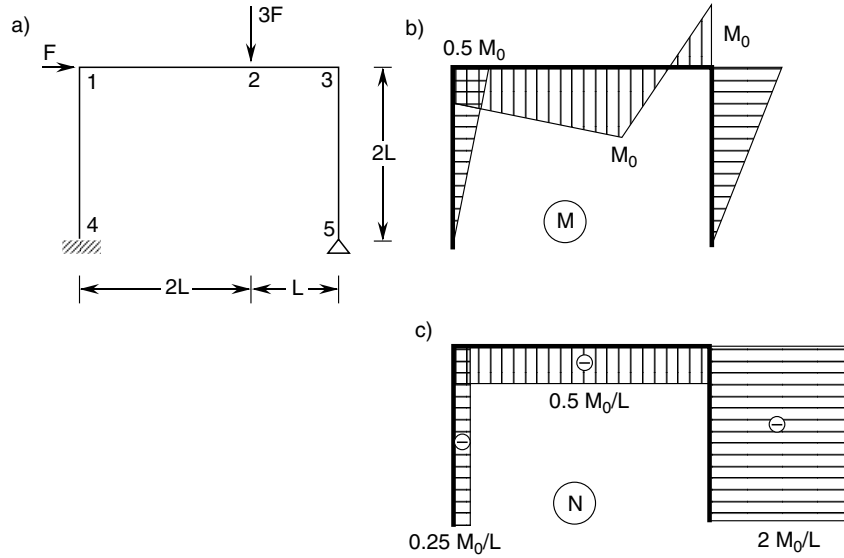


Figure 13.12 Frame from Example 13.3

considerations are given in Figure 13.12(c). According to the theory neglecting the effect of normal forces, the structure collapses when  $\hat{F}_0 = 0.75M_0/L$ . For each critical cross section  $ij$  we determine a scaling factor  $\xi_{ij}$  such that the internal forces  $N_{ij}$  and  $M_{ij}$  multiplied by  $\xi_{ij}$  are plastically admissible; cf. (13.49). From

$$\frac{\xi_{ij}|N_{ij}|}{N_0} + \frac{\xi_{ij}|M_{ij}|}{M_0} = 1 \quad (13.52)$$

we get

$$\xi_{ij} = \frac{1}{n_{ij} + m_{ij}} \quad (13.53)$$

where

$$n_{ij} = |N_{ij}|/N_0 \quad (13.54)$$

$$m_{ij} = |M_{ij}|/M_0 \quad (13.55)$$

For example, for cross section 12 we have

$$n_{12} = |N_{12}|/N_0 = 0.5M_0/LN_0 = 0.5h_0/L \quad (13.56)$$

$$m_{12} = |M_{12}|/M_0 = 0.5M_0/M_0 = 0.5 \quad (13.57)$$

$$\xi_{12} = \frac{1}{0.5h_0/L + 0.5} = \frac{2}{1 + h_0/L} \quad (13.58)$$

For an ideal sandwich, the parameter  $h_0 = M_0/N_0 = W_0/A$  is equal to  $h/2$  where  $h$  is the depth of the cross section. For physically meaningful (i.e. positive) values of  $h_0$ , the scaling factor  $\xi_{12}$  is clearly always greater than one, which means that the internal forces at this cross section are plastically admissible even without rescaling. The other cross sections can be processed similarly; see Table 13.1.

**Table 13.1** Normalized internal forces at critical cross sections

$ij$	$n_{ij}L/h_0$	$m_{ij}$
14	0.25	0.5
12	0.5	0.5
23	0.5	1
32	0.5	1
35	2	1

The smallest value of the scaling factor is obviously obtained at cross section 35, i.e. at the top of the right column. This is true for any ratio  $h_0/L$ . The resulting safety reduction factor is

$$\xi_{min} = \min_{ij} \xi_{ij} = \xi_{35} = \frac{1}{1 + 2h_0/L} \quad (13.59)$$

As might have been expected, for  $h_0/L \rightarrow 0$  we obtain  $\xi_{min} \rightarrow 1$ , which is the limit case in which the effect of axial forces vanishes. This is, of course, true only in the context of a geometrically linear theory that neglects the second-order effects of deflections on the distribution of internal forces. For slender columns, these effects must be taken into account, and then the role of the normal force becomes important.

For the ratio  $h/2L = 1 : 10$ , the safety reduction factor is

$$\xi_{min} = \frac{1}{1 + 2h_0/L} = \frac{1}{1 + h/L} = \frac{1}{1 + 0.2} = 0.833 \quad (13.60)$$

This means that the collapse load is no smaller than

$$F_s = \xi_{min} \hat{F}_0 = 0.833 \times 0.75 \frac{M_0}{L} = 0.625 \frac{M_0}{L} \quad (13.61)$$

The reduction of the ultimate load by 17% is already appreciable. However, this is only a conservative, crude estimate. The exact safety factor will be evaluated in Example 13.5.  $\square$

The ideal sandwich is an extreme case in the sense that, for given  $N_0$  and  $M_0$ , its plastic limit envelope is the smallest possible plastic limit envelope. This readily follows from the property of convexity. The parallelogram may thus be used as a safe approximation of the plastic limit envelope for a cross section of any shape. As we always have  $m_{ij} \leq 1$  (otherwise the condition of plastic admissibility under pure bending would be violated), we can write

$$\xi_{ij} = \frac{1}{n_{ij} + m_{ij}} \geq \frac{1}{n_{ij} + 1} \geq 1 - n_{ij} \quad (13.62)$$

and

$$\mu_0 \geq \xi_{min} \hat{\mu}_0 \geq \hat{\mu}_0 \left( 1 - \max_{ij} \frac{|N_{ij}|}{N_0} \right) \quad (13.63)$$

Albeit very crude, this is a universally applicable safe estimate of the safety factor (i.e. an estimate preserving a lower bound). For example, if the normal forces calculated

for the standard model (i.e. the model with plastic hinges affected only by bending moments) nowhere exceed 10% of the plastic axial force, we can be sure that the reduction of the safety factor due to the effect of normal forces is not greater than 10%.

The behavior of frames with members of a rectangular cross section is sensitive to the effect of normal forces much less than is the behavior of an ideal sandwich. The shape of the plastic limit envelope is parabolic, and therefore the bending moment carried by the cross section decreases more slowly as the normal force increases. The yield condition

$$\left(\frac{\xi N}{N_0}\right)^2 + \frac{\xi |M|}{M_0} = 1 \quad (13.64)$$

leads to a quadratic equation

$$n^2 \xi^2 + m \xi - 1 = 0 \quad (13.65)$$

for the scaling factor  $\xi$ . The solution

$$\xi = \frac{\sqrt{m^2 + 4n^2} - m}{2n^2} \quad (13.66)$$

can safely be estimated as

$$\xi \geq 1 - n^2 \quad (13.67)$$

This means that, for a rectangular section, we have

$$\mu_0 \geq \hat{\mu}_0 \left(1 - \max_{ij} \frac{N_{ij}^2}{N_0^2}\right) \quad (13.68)$$

For example, if the normal forces do not exceed 20% of the plastic axial force, the reduction of the safety factor is at most 4%. It should be emphasized that estimate (13.68) is valid only if all critical sections are rectangular, while estimate (13.63) is universally applicable. The behavior of massive cross sections is closer to the rectangular section while thin-walled cross sections is closer to the ideal sandwich. Thus, the latter are more sensitive to the effect of normal forces.

#### 13.4 APPLICATION OF LINEAR PROGRAMMING

As already mentioned, the yield conditions derived by taking into account the interaction of bending moments and normal forces are typically nonlinear. Linear programming techniques can only be applied to such models if the yield conditions are linearized.

For this purpose we may replace the curvilinear yield surface by a polygon. The equations describing the sides of the polygon are obviously linear with respect to  $N$  and  $M$ . To preserve the applicability of the bound theorems, it is necessary to use interior and exterior approximations, i.e. linearized yield surfaces that lie totally inside or outside the exact yield surface. Examples of the interior and exterior approximations are shown in Figure 13.13. With regard to the approximate yield surface consisting of straight line segments, it is interesting to note that it represents

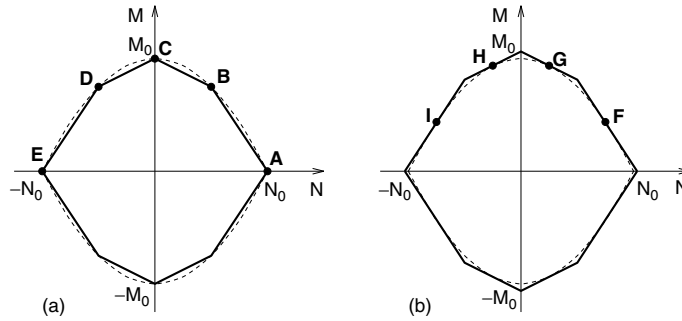


**Figure 13.13** Linearization of the plastic limit envelope: a) interior approximation, b) exterior approximation

the exact yield surface for an idealized cross section that has no web and a finite number of thin horizontal flanges.

Consider first the interior approximation (Figure 13.13(a)). Let  $\mu_0$  denote the exact safety factor for the actual yield surface, and let  $\mu_{\text{int}}$  denote the safety factor based on approximate yield surfaces that lie in the interior of the actual ones (for each critical cross section). Every stress state statically admissible with respect to the interior approximation is also statically admissible for the actual yield surface. This means that any lower bound  $\mu_{\text{int},s}$  on the approximate safety factor  $\mu_{\text{int}}$  is at the same time a lower bound on the exact safety factor,  $\mu_0$ .

Next, consider the exterior approximation (Figure 13.13(b)). Let  $\mu_{\text{ext}}$  denote the safety factor for the approximate yield surface lying outside the actual one. Now the situation is the opposite – the actual internal forces at collapse are statically admissible for the exterior approximation, and so  $\mu_0 \leq \mu_{\text{ext}}$ . Furthermore, any kinematically admissible multiplier  $\mu_{\text{ext},k}$  based on the exterior approximation is greater than or equal to the exact safety factor  $\mu_{\text{ext}}$  for the exterior approximation, according to the upper bound theorem applied to the exterior approximation. Hence, the upper bound is preserved.

The previous conclusions are summarized in the inequality

$$\mu_{\text{int},s} \leq \mu_{\text{int}} \leq \mu_0 \leq \mu_{\text{ext}} \leq \mu_{\text{ext},k} \quad (13.69)$$

Of course, this does not mean that the interior approximation must be used exclusively with the static approach, nor that the exterior approximation must be used exclusively with the kinematic approach. We can, for example, compute  $\mu_{\text{int}}$  by the kinematic approach, however, keeping in mind that the intermediate values  $\mu_{\text{int},k}$  do not provide any bounds on the exact safety factor  $\mu_0$ . Only the optimal value  $\mu_{\text{int}} = \min \mu_{\text{int},k}$  is a *lower* bound on  $\mu_0$ .

After a slight generalization, the linear programming formulations developed in previous chapters are applicable to frames with generalized plastic hinges. In the *static formulation*, it is no longer possible to write the conditions of plastic admissibility simply as  $|\mathbf{s}| \leq \mathbf{s}_0$ . Every nonlinear condition of plastic admissibility at a critical cross section,  $f(N, M) \leq 0$ , will be replaced by several linearized conditions, each of which involves two internal forces – the bending moment and the normal force. Without any loss of generality, we can describe such conditions by a linear inequality

$$a \frac{N}{N_0} + b \frac{M}{M_0} \leq 1 \quad (13.70)$$

or

$$ah_0N + bM \leq M_0 \quad (13.71)$$

where  $a$  and  $b$  are dimensionless coefficients and  $h_0 = M_0/N_0$ . We can always write the condition of plastic admissibility with a positive right-hand side and with the 'less than or equal to' sign because the stress-free state,  $N = 0$  and  $M = 0$ , must always be inside the elastic domain. The complete system of linearized conditions of plastic admissibility can be written as

$$\mathbf{Y} \mathbf{s} \leq \tilde{\mathbf{s}}_0 \quad (13.72)$$

where matrix  $\mathbf{Y}$  contains the coefficients  $ah_0$  and  $b$  multiplying individual internal forces in the linearized conditions of plastic admissibility, and column matrix  $\tilde{\mathbf{s}}_0$  contains the corresponding terms  $M_0$  on the right-hand side. Note that  $\tilde{\mathbf{s}}_0$  now contains one entry per linearized condition of plastic admissibility, and so the value  $M_{0,ij}$  is repeated many times for every critical cross section  $ij$ . The notation with a superposed tilda should emphasize the difference compared to the column matrix  $\mathbf{s}_0$ , which contains only one entry per cross section.

It is useful to derive general expressions describing the segments of the linearized yield surface. The *interior approximation* is usually constructed by connecting selected points located on the exact yield surface. Due to convexity, the resulting polygon is guaranteed to lie inside the exact yield surface. Let  $(\bar{N}_1, \bar{M}_1)$  and  $(\bar{N}_2, \bar{M}_2)$  be two points on the exact yield surface. Denoting  $\bar{n}_i = \bar{N}_i/N_0$ ,  $\bar{m}_i = \bar{M}_i/M_0$ ,  $i = 1, 2$ , and solving the system of linear equations

$$a\bar{n}_1 + b\bar{m}_1 = 1 \quad (13.73)$$

$$a\bar{n}_2 + b\bar{m}_2 = 1 \quad (13.74)$$

for unknowns  $a$  and  $b$ , we obtain

$$a = \frac{\bar{m}_2 - \bar{m}_1}{c}, \quad b = \frac{\bar{n}_1 - \bar{n}_2}{c} \quad \text{where } c = \bar{n}_1\bar{m}_2 - \bar{n}_2\bar{m}_1 \quad (13.75)$$

The *exterior approximation* usually consists of segments that are tangent to the exact yield surface. Again, convexity implies that the exact yield surface is fully contained in the resulting polygon. Suppose that we want to describe a segment that is tangential to the nonlinear yield surface at a certain point  $(\bar{N}, \bar{M})$ . Let us denote by

$$\bar{f}_{,N} \equiv \frac{\partial f}{\partial N}(\bar{N}, \bar{M}), \quad \bar{f}_{,M} \equiv \frac{\partial f}{\partial M}(\bar{N}, \bar{M}) \quad (13.76)$$

the components of the gradient of the yield function at the given point. The tangent line must be orthogonal to the gradient vector and pass through point  $(\bar{N}, \bar{M})$ , and so it is described by

$$\bar{f}_{,N}(N - \bar{N}) + \bar{f}_{,M}(M - \bar{M}) = 0 \quad (13.77)$$

After assembling the constant terms at the right-hand side and rescaling, we can cast (13.77) in the format of (13.70) with

$$a = \frac{N_0\bar{f}_{,N}}{c}, \quad b = \frac{M_0\bar{f}_{,M}}{c}, \quad \text{where } c = \bar{f}_{,N}\bar{N} + \bar{f}_{,M}\bar{M} \quad (13.78)$$

It can be proven that  $c$  is always positive, and so the denominator in the expressions for  $a$  and  $b$  cannot vanish; see Problem 13.3.

**Example 13.4:** Set up the linearized conditions of plastic admissibility for a rectangular cross section corresponding to a) the interior approximation in Figures 13.13(a),(b) the exterior approximation in Figure 13.13(b).

**Solution:** a) The normalized coordinates of points A to E from Figure 13.13(a) are listed in Table 13.2(a). Consider for example the condition corresponding to segment CB. Substituting  $\bar{n}_1 = 0$ ,  $\bar{m}_1 = 1$ ,  $\bar{n}_2 = 0.5$  and  $\bar{m}_2 = 0.75$  into (13.75), we obtain  $a = 0.5$  and  $b = 1$ . Consequently, the linearized condition of plastic admissibility (13.71) is

$$0.5h_0N + M \leq M_0 \quad (13.79)$$

The remaining segments of the octagon approximating the plastic limit envelope can be processed in a similar manner. The resulting set of inequalities (13.72) reads

$$\begin{bmatrix} 0.5h_0 & 1 \\ h_0 & 0.667 \\ 0.5h_0 & -1 \\ h_0 & -0.667 \\ -0.5h_0 & -1 \\ -h_0 & -0.667 \\ -0.5h_0 & 1 \\ -h_0 & 0.667 \end{bmatrix} \begin{Bmatrix} N \\ M \end{Bmatrix} \leq \begin{Bmatrix} M_0 \\ M_0 \\ M_0 \\ M_0 \\ M_0 \\ M_0 \\ M_0 \\ M_0 \end{Bmatrix} \quad (13.80)$$

b) Differentiation of the yield function  $f(N, M) = (N/N_0)^2 + |M|/M_0 - 1$  that corresponds to a rectangular section yields

$$f_{,N} \equiv \frac{\partial f}{\partial N} = \frac{2N}{N_0^2}, \quad f_{,M} \equiv \frac{\partial f}{\partial M} = \frac{\text{sgn } M}{M_0} \quad (13.81)$$

The normalized coordinates of points F to I from Figure 13.13(b) and the corresponding gradient components are listed in Table 13.2(b). Consider for example the condition corresponding to the tangent at point F. Substituting  $\bar{N} = 0.75N_0$ ,  $\bar{M} = 0.4375M_0$ ,  $\bar{f}_{,N} = 1.5/N_0$  and  $\bar{f}_{,M} = 1/M_0$  into (13.78), we obtain  $c = 1.5625$ ,  $a = 0.96$  and  $b = 0.64$ . Consequently, the linearized condition of plastic admissibility (13.71) is

$$0.96h_0N + 0.64M \leq M_0 \quad (13.82)$$

The remaining segments of the octagon approximating the plastic limit envelope can be processed in a similar manner. The resulting set of inequalities (13.72) reads

$$\begin{bmatrix} 0.4706h_0 & 0.9412 \\ 0.96h_0 & 0.64 \\ 0.4706h_0 & -0.9412 \\ 0.96h_0 & -0.64 \\ -0.4706h_0 & -0.9412 \\ -0.96h_0 & -0.64 \\ -0.4706h_0 & 0.9412 \\ -0.96h_0 & 0.64 \end{bmatrix} \begin{Bmatrix} N \\ M \end{Bmatrix} \leq \begin{Bmatrix} M_0 \\ M_0 \\ M_0 \\ M_0 \\ M_0 \\ M_0 \\ M_0 \\ M_0 \end{Bmatrix} \quad (13.83)$$

□

**Table 13.2** Points on the exact yield surface serving as a basis of the a) interior approximation, b) exterior approximation

point	$n = \frac{N}{N_0}$	$m = \frac{M}{M_0}$
A	1	0
B	0.5	0.75
C	0	1
D	-0.5	0.75
E	-1	0

point	$n = \frac{N}{N_0}$	$m = \frac{M}{M_0}$	$N_0 \bar{f}_{,N}$	$M_0 \bar{f}_{,M}$
F	0.75	0.4375	1.5	1
G	0.25	0.9375	0.5	1
H	-0.25	0.9375	-0.5	1
I	-0.75	0.4375	-1.5	1

(a)

(b)

In the *kinematic formulation*, it is not convenient to express the dissipation rate directly in terms of the generalized strain rates. Suppose that we know on which segment of the linearized yield surface plastic flow takes place. Vector  $\{ah_0, b\}^T$  is the gradient of the linear yield function  $f(N, M) = ah_0N + bM - M_0$  associated with condition (13.71), and so it is an outward normal to the corresponding segment. Due to normality, the plastic flow can be described by

$$\begin{Bmatrix} \dot{\epsilon}_p \\ \dot{\theta} \end{Bmatrix} = \dot{\lambda} \begin{Bmatrix} ah_0 \\ b \end{Bmatrix} \quad (13.84)$$

where  $\dot{\lambda} \geq 0$  is the rate of a scalar variable called the *plastic multiplier*. The dissipation rate is now easily evaluated as

$$D_{\text{int}} = N\dot{\epsilon}_p + M\dot{\theta} = (ah_0N + bM)\dot{\lambda} = M_0\dot{\lambda} \quad (13.85)$$

In the last step, we have exploited the fact that during plastic flow the yield condition must be satisfied, and so  $ah_0N + bM = M_0$ . If the active segment of the yield surface is not known *a priori*, we express the plastic deformation rates by a linear combination

$$\dot{\epsilon}_p = \sum_i \mathbf{n}_i \dot{\lambda}_i = \mathbf{N} \dot{\boldsymbol{\lambda}} \quad (13.86)$$

where the columns of  $\mathbf{N}$  (vectors  $\mathbf{n}_i$ ) are outward normal vectors to the yield surface constructed at individual straight segments, and  $\dot{\boldsymbol{\lambda}} \geq \mathbf{0}$  is the vector of rates of the corresponding plastic multipliers.

As we have seen, the coefficients of the linearized condition of plastic admissibility (13.71) associated with a certain segment are at the same time components of a vector normal to this segment. Recall that the coefficients of plastic admissibility conditions form the rows of matrix  $\mathbf{Y}$ , and that the components of normals to the yield surface form the columns of matrix  $\mathbf{N}$ . With a proper ordering, we have  $\mathbf{Y} = \mathbf{N}^T$ , and then the linearized conditions of plastic admissibility (13.72) read

$$\mathbf{N}^T \mathbf{s} \leq \tilde{\mathbf{s}}_0 \quad (13.87)$$

The rate of a certain plastic multiplier can be nonzero only if the corresponding yield condition is satisfied. This statement, mathematically written as

$$(\mathbf{N}^T \mathbf{s} - \tilde{\mathbf{s}}_0)^T \dot{\boldsymbol{\lambda}} = 0 \quad (13.88)$$

is one of the Karush–Kuhn–Tucker conditions, to be discussed in Section 15.2.4. The dissipation rate can now be expressed as a function of the plastic multiplier rates,

$$D_{\text{int}} = \mathbf{s}^T \dot{\mathbf{e}}_p = \mathbf{s}^T \mathbf{N} \dot{\boldsymbol{\lambda}} = (\mathbf{N}^T \mathbf{s})^T \dot{\boldsymbol{\lambda}} = \tilde{\mathbf{s}}_0^T \dot{\boldsymbol{\lambda}} \quad (13.89)$$

This is obviously a generalization of (13.85). It is important to realize that the *independent* variables characterizing the plastic flow are now  $\dot{\boldsymbol{\lambda}}$  and not  $\dot{\mathbf{e}}_p$ . The dissipation rate is uniquely determined by  $\dot{\boldsymbol{\lambda}}$  because  $\tilde{\mathbf{s}}_0$  is a given constant vector. By contrast to that, the rates of plastic generalized strains  $\dot{\mathbf{e}}_p$  in the expression  $D_{\text{int}} = \mathbf{s}^T \dot{\mathbf{e}}_p$  are multiplied by the internal forces  $\mathbf{s}$  that are not known *a priori* and not always uniquely determined by  $\dot{\mathbf{e}}_p$ . Moreover, the elastic domain can be unbounded for certain cases (e.g. for an idealized material that yields only in tension, but not in compression), and then some combinations of plastic generalized strains may be inadmissible.

We have prepared all the prerequisites for the formulation of limit analysis of frames with generalized plastic hinges in the format of linear programming. Now we briefly present the two fundamental approaches.

**Static approach:** A statically admissible state is defined by plastically admissible internal forces that are in equilibrium with a certain multiple of the reference loading. According to the lower bound theorem of limit analysis, the safety factor is obtained by maximizing the statically admissible load multiplier. This can be stated as a problem of linear programming

$$\text{Maximize } g(\mathbf{s}, \mu_s) \equiv \mu_s \quad (13.90)$$

subject to

$$\mathbf{B}^T \mathbf{s} - \bar{\mathbf{f}} \mu_s = \mathbf{0} \quad (13.91)$$

$$\mathbf{N}^T \mathbf{s} \leq \tilde{\mathbf{s}}_0 \quad (13.92)$$

**Kinematic approach:** A kinematically admissible state is defined by a collapse mechanism that satisfies the conditions of compatibility and leads to a positive external power supplied by the reference loading. According to the upper bound theorem of limit analysis, the safety factor is obtained by minimizing the kinematically admissible load multiplier. This can be stated as a problem of linear programming

$$\text{Minimize } f(\dot{\boldsymbol{\lambda}}, \dot{\mathbf{d}}) \equiv \tilde{\mathbf{s}}_0^T \dot{\boldsymbol{\lambda}} \quad (13.93)$$

subject to

$$\mathbf{N} \dot{\boldsymbol{\lambda}} - \mathbf{B} \dot{\mathbf{d}} = \mathbf{0} \quad (13.94)$$

$$\bar{\mathbf{f}}^T \dot{\mathbf{d}} = 1 \quad (13.95)$$

$$\dot{\boldsymbol{\lambda}} \geq \mathbf{0} \quad (13.96)$$

The reader can verify that the static formulation (13.90)–(13.92) is the dual of the kinematic formulation (13.93)–(13.96), and vice versa; see Problem 13.4.

The linear programming problem in (13.93)–(13.96) is a generalization of problem (7.7)–(7.11), which ensued from the simplified method. We will convert it to the standard form using a similar technique as in Section 7.2. The displacement rates can be eliminated by applying appropriate Gauss transformations to the kinematic relations (13.94). This process can formally be described using matrices  $\mathbf{S}$  and  $\mathbf{P}$  introduced in Figure 7.2, which have the following properties:

$$\mathbf{S}^T \mathbf{B} = \mathbf{O} \quad (13.97)$$

$$\mathbf{P}^T \mathbf{B} = \mathbf{I} \quad (13.98)$$

Multiplying (13.94) from the left respectively by  $\mathbf{S}$  and  $\mathbf{P}$  leads to

$$\mathbf{S}^T \mathbf{N} \dot{\boldsymbol{\lambda}} = \mathbf{0} \quad (13.99)$$

$$\mathbf{P}^T \mathbf{N} \dot{\boldsymbol{\lambda}} = \dot{\mathbf{d}} \quad (13.100)$$

Physically, (13.99) are the compatibility conditions, and (13.100) are the expressions for the displacement rates in terms of the plastic multiplier rates. Substituting (13.100) into (13.95) we eliminate the displacement rates from the problem and arrive at the standard form

$$\text{Minimize } f(\dot{\boldsymbol{\lambda}}) \equiv \tilde{\mathbf{s}}_0^T \dot{\boldsymbol{\lambda}} \quad (13.101)$$

subject to

$$\mathbf{S}^T \mathbf{N} \dot{\boldsymbol{\lambda}} = \mathbf{0} \quad (13.102)$$

$$\bar{\mathbf{f}}^T \mathbf{P}^T \mathbf{N} \dot{\boldsymbol{\lambda}} = 1 \quad (13.103)$$

$$\dot{\boldsymbol{\lambda}} \geq \mathbf{0} \quad (13.104)$$

Of course, when the problem is solved by hand we do not have to perform all the matrix manipulations because the conditions of compatibility and the expressions for the displacement rates can be constructed directly using the principle of virtual work.

**Example 13.5:** Evaluate the safety factor for the structure in Figure 13.14(a). Take into account the effect of normal forces. The cross section is a rectangle of depth  $h = L/8$ .

**Solution:** The structure is twice statically indeterminate, and so the failure mechanism involves three plastic hinges. First let us neglect the effect of axial forces. Elementary limit analysis easily reveals the failure mechanism in Figure 13.14(b); the corresponding distribution of the bending moments and normal forces is plotted in Figures 13.14(c), (d). According to the simplified theory taking into account only the effect of bending moments, the structure would fail at  $\hat{F} = 2.5M_0/L$ .

Note that the simplified condition of plastic admissibility,  $|M| \leq M_0$ , can be regarded as an exterior approximation of the ‘exact’ condition,  $(N/N_0)^2 + |M|/M_0 \leq 1$ ; see Figure 13.15(a). Consequently, the safety factor evaluated from the simplified theory is an upper bound on the actual safety factor. We can construct a crude lower bound using the technique explained in Section 13.3. The internal forces corresponding

**Table 13.3** Internal forces and scaling factors at critical cross sections (simplified solution)

$ij$	$M_{ij}/M_0$	$N_{ij}/N_0$	$\xi_{ij}$	$\xi_{ij}M_{ij}/M_0$	$\xi_{ij}N_{ij}/N_0$
21	-1.0	0.375	0.889	-0.889	0.333
32	0.5	0.375	$> 1$		
34	-0.5	-0.250	$> 1$		
45	-1.0	-0.250	0.944	-0.944	-0.236
54	-1.0	-0.250	0.944	-0.944	-0.236

to the simplified solution and the scaling factors that bring them back to the plastic limit envelope are listed in Table 13.3; see also Figure 13.15(b). We consider cross sections 32 and 34 separately because they carry different normal forces. On the other hand, at each of nodes 2, 4 and 5 we have to inspect only one critical cross section. The smallest reduction factor  $\xi_{min} = \min \xi_{ij} = \xi_{21} = 0.889$  multiplied by  $\hat{F}$  gives a lower bound on the safety factor  $F_0$ . Now we can bracket the safety factor by

$$0.889\hat{F} \leq F_0 \leq \hat{F}, \quad \text{i.e.} \quad 2.222\frac{M_0}{L} \leq F_0 \leq 2.5\frac{M_0}{L} \quad (13.105)$$

In order to improve this estimate, we will solve the problem using a more accurate approximation of the nonlinear yield surface. In general, we should replace the yield surface by a polygon that matches it as closely as possible. Each side of the polygon at each critical cross section is associated with one plastic multiplier, and so the number of unknowns in the linear programming problem (13.101)–(13.104) rapidly increases as the polygon approaches the nonlinear interaction diagram. Typically, however, only one plastic multiplier per active yield hinge is nonzero (or at most two

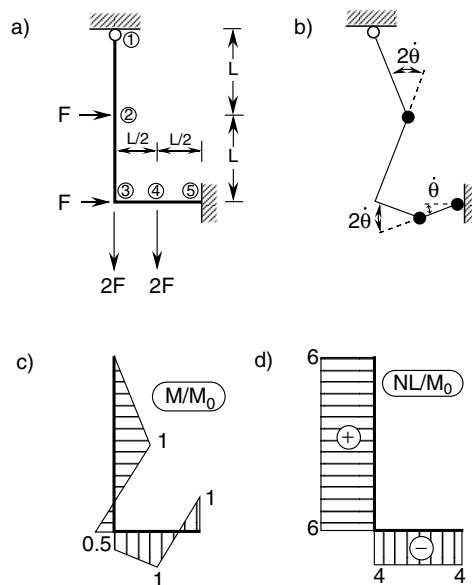


**Figure 13.14** Simplified solution of Example 13.5

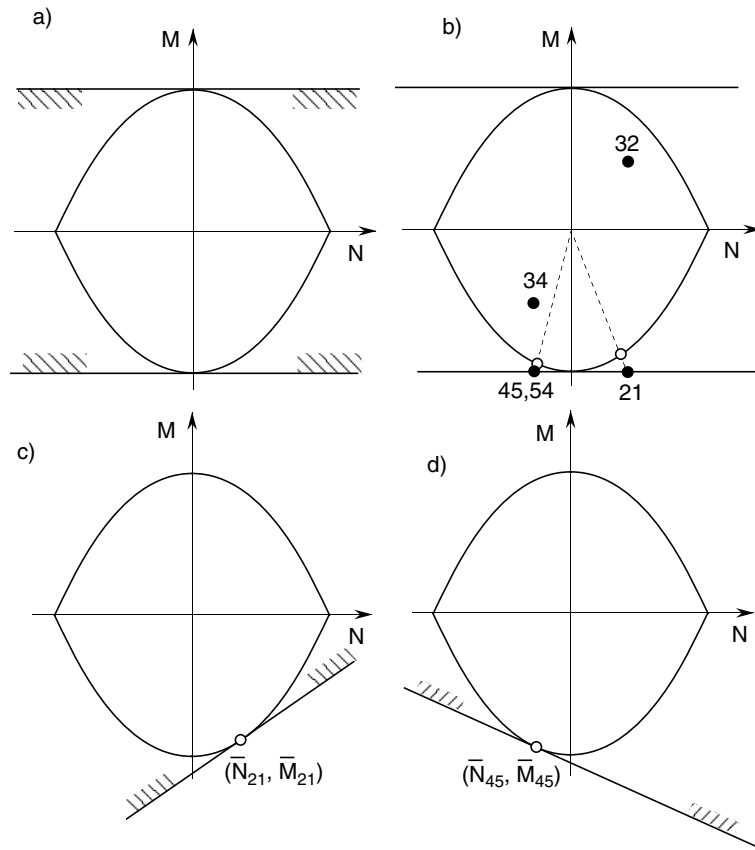


**Figure 13.15** Scaling to limit envelope and approximation of yield conditions

if the corresponding point in the interaction diagram is located in a corner of the polygon). The simplified solution, neglecting the effect of normal forces, gives us a clue regarding the segments of the polygons on which plastic flow is expected to take place. We can assume that the actual values of internal forces at collapse will not be too far from the scaled values computed by the simplified method. Therefore, we can dramatically reduce the number of unknowns in our problem by taking into account only one plastic multiplier per critical cross section. This multiplier corresponds to plastic flow taking place in the direction determined by the normal to the interaction curve at the point representing the scaled internal forces from the simplified solution. In other words, we approximate the nonlinear elastic domain of internal forces by a halfplane bounded by a tangent to the actual domain; see Figures 13.15(c),(d). Such an approximation is in general very crude, but the results are excellent if the actual and simplified solutions are not too far apart. We can even assume that plastic hinges will form at the same cross sections as for the simplified solution, and then the number of unknowns further decreases. For the present problem, we introduce only three plastic multipliers corresponding to cross sections 21, 45 and 54. The ratio between the rate of plastic rotation and plastic extension at each plastic hinge is determined by the flow rule. For example, for cross section 21 the internal forces estimated by the simplified method and scaled to the yield surface are  $\bar{N}_{21} = \xi_{21}N_{21} = 0.333N_0$  and  $\bar{M}_{21} = \xi_{21}M_{21} = -0.889M_0$ . Substituting this into expressions (13.81) for the

gradient components of the yield function we get

$$\bar{f}_{,N} = \frac{2\bar{N}}{N_0^2} = \frac{2 \times 0.333N_0}{N_0^2} = \frac{0.667}{N_0} \quad (13.106)$$

$$\bar{f}_{,M} = \frac{\text{sgn } \bar{M}}{M_0} = \frac{\text{sgn}(-0.889)}{M_0} = -\frac{1}{M_0} \quad (13.107)$$

and then formulae (13.78) furnish  $c = 1.111$ ,  $a = 0.6$  and  $b = -0.9$ . The linearized condition of plastic admissibility (13.71) at cross section 21 is thus

$$0.6h_0N_{21} - 0.9M_{21} \leq M_0 \quad (13.108)$$

and the flow rule (13.84) gives

$$\dot{e}_{p,21} = 0.6h_0\dot{\lambda}_{21} \quad (13.109)$$

$$\dot{\theta}_{21} = -0.9\dot{\lambda}_{21} \quad (13.110)$$

In a completely analogous manner, we get the expressions for the deformation rates at cross sections 45 and 54,

$$\dot{e}_{p,45} = -0.4472h_0\dot{\lambda}_{45} \quad (13.111)$$

$$\dot{\theta}_{45} = -0.9472\dot{\lambda}_{45} \quad (13.112)$$

$$\dot{e}_{p,54} = -0.4472h_0\dot{\lambda}_{54} \quad (13.113)$$

$$\dot{\theta}_{54} = -0.9472\dot{\lambda}_{54} \quad (13.114)$$

Now we could easily construct the matrix  $\mathbf{N}$  and set up the linear programming problem (13.93)–(13.96). The kinematic matrix  $\mathbf{B}$  would contain only the rows corresponding to the generalized strains of interest, i.e.  $\dot{e}_{p,21}$ ,  $\dot{\theta}_{21}$ ,  $\dot{e}_{p,45}$ ,  $\dot{\theta}_{45}$ ,  $\dot{e}_{p,54}$  and  $\dot{\theta}_{54}$ . Instead of setting up and transforming the kinematic relations (13.94), we will directly construct the conditions of compatibility (13.99) and expressions (13.100), which lead to the standard form (13.101)–(13.104).

The structure is twice statically indeterminate, and so we need to find two independent compatibility conditions. Figure 13.16 shows a primary structure subjected to two loading cases in which we apply unit values of the redundants. This provides us with two independent self-equilibrated states of internal forces. According to the principle of virtual work, the work of these forces on the actual deformations must vanish (because no virtual external forces are applied on the original structure). In this way we obtain the compatibility conditions

$$-\dot{e}_{p,21}/L + 0.5\dot{\theta}_{21} - 0.5\dot{e}_{p,45}/L - 0.5\dot{\theta}_{45} - 0.5\dot{e}_{p,54}/L = 0 \quad (13.115)$$

$$\dot{e}_{p,21}/L - 0.5\dot{\theta}_{45} + \dot{\theta}_{54} = 0 \quad (13.116)$$

Note that it was essential to include the virtual work of the normal forces, since otherwise we would have obtained the compatibility conditions of the simplified method, which neglects the axial plastic deformations. Multiplying by  $2L$  and substituting expressions (13.109)–(13.114), we express the conditions of compatibility in terms of the plastic multiplier rates:

$$(-0.9L - 1.2h_0)\dot{\lambda}_{21} + (0.9472L + 0.4472h_0)\dot{\lambda}_{45} + 0.4472h_0\dot{\lambda}_{54} = 0 \quad (13.117)$$

$$1.2h_0\dot{\lambda}_{21} + 0.9472L\dot{\lambda}_{45} - 1.8944L\dot{\lambda}_{54} = 0 \quad (13.118)$$

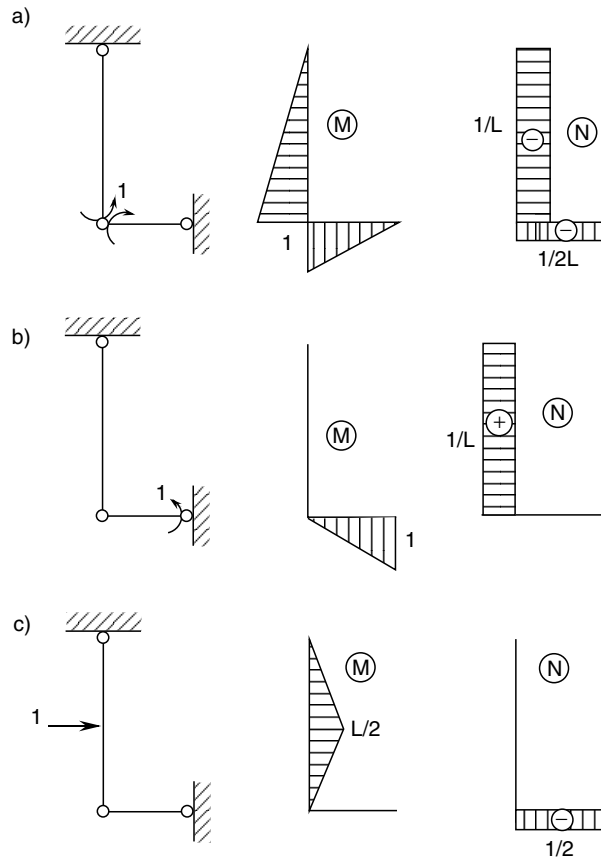


**Figure 13.16** Virtual states considered in Example 13.5

We have two conditions for three unknown plastic multiplier rates, which is correct because the assumed mechanism should have one degree of freedom. We select one unknown, say  $\dot{\lambda}_{54}$ , as an independent one, and express the two remaining unknowns by standard elimination. This would be too tedious in the general symbolic form with arbitrary  $L$  and  $h_0$ . Therefore, we continue the calculation with the given ratio  $h_0 : L = h : 2L = 1 : 16$ . After elimination we get

$$\dot{\lambda}_{21} = 1.8801\dot{\lambda}_{54} \tag{13.119}$$

$$\dot{\lambda}_{45} = 1.8511\dot{\lambda}_{54} \tag{13.120}$$

Note that both coefficients in the resulting expressions are positive, for if they were not, it would be impossible to satisfy the condition that all plastic multiplier rates be nonnegative, and the assumed mechanism would not be kinematically admissible. The dissipation rate can now be expressed in terms of the independent plastic multiplier rate as

$$D_{\text{int}} = M_0(\dot{\lambda}_{21} + \dot{\lambda}_{45} + \dot{\lambda}_{54}) = 4.731M_0\dot{\lambda}_{54} \tag{13.121}$$

We also need to express the rates of displacements on which work is being done by external forces in terms of the plastic multiplier rates. First, we use the principle of virtual work to express them in terms of the nonzero deformation rates. For example,

the unit virtual state in Figure 13.16(c) leads to

$$\dot{u}_2 = -0.5L\dot{\theta}_{21} - 0.5\dot{e}_{45} - 0.5\dot{e}_{54} \quad (13.122)$$

In a similar fashion, we obtain expressions for the other displacement rates of interest,

$$\dot{u}_3 = -\dot{e}_{45} - \dot{e}_{54} \quad (13.123)$$

$$\dot{w}_3 = \dot{e}_{21} \quad (13.124)$$

$$\dot{w}_4 = -0.25L\dot{\theta}_{45} + 0.5\dot{e}_{21} \quad (13.125)$$

Using (13.109)–(13.114) and then (13.119)–(13.120), we obtain

$$\dot{u}_2 = 0.8859L\dot{\lambda}_{54} \quad (13.126)$$

$$\dot{u}_3 = 0.0797L\dot{\lambda}_{54} \quad (13.127)$$

$$\dot{w}_3 = 0.0705L\dot{\lambda}_{54} \quad (13.128)$$

$$\dot{w}_4 = 0.4736L\dot{\lambda}_{54} \quad (13.129)$$

The external power done by the kinematically admissible external forces is

$$\dot{W}_{\text{ext}} = F_k\dot{u}_2 + F_k\dot{u}_3 + 2F_k\dot{w}_3 + 2F_k\dot{w}_4 = 2.054F_kL\dot{\lambda}_{54} \quad (13.130)$$

Finally, combining (13.121) and (13.130) into the power equality, we get an improved kinematically admissible load

$$F_k = \frac{4.731M_0}{2.054L} = 2.303\frac{M_0}{L} \quad (13.131)$$

To keep the derivations easy to follow, we were showing only four significant digits for all the intermediate results. When the calculation is performed with a high accuracy, the final value of the kinematically admissible load is  $F_k = 2.303645M_0/L$ . Now we can evaluate the corresponding internal forces from equilibrium and normality conditions. As expected, the bending moments and normal forces at the yield hinges are not too different from the scaled values from the simplified solution. The results are plotted in Figure 13.17 and listed in Table 13.4, which shows also the scaling factors needed to bring the internal forces back to the exact yield surface. Their values indicate that the improved upper bound is very accurate. Internal forces at sections 32 and 34 still remain inside the elastic domain, which means that the assumed locations of plastic hinges have been chosen correctly. The smallest scaling factor is  $\xi_{\min} = 0.999989$ , and so the relative error of the upper bound is about  $10^{-5}$ . The collapse load can be bracketed as

$$0.999989F_k \leq F_0 \leq F_k \quad (13.132)$$

$$2.303567\frac{M_0}{L} \leq F_0 \leq 2.303645\frac{M_0}{L} \quad (13.133)$$

There is no need for further improvement of this estimate. If the results were less accurate, we could repeat the entire procedure, starting from the construction of new tangent lines to the interaction diagram. Note that, in this example, the presence of

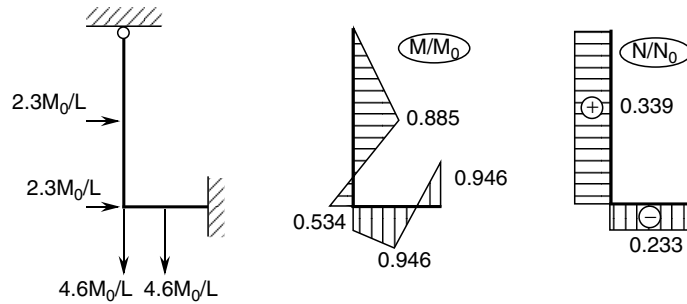


Figure 13.17 Internal forces at collapse

Table 13.4 Internal forces and scaling factors at critical sections (improved solution)

$ij$	$M_{ij}/M_0$	$N_{ij}/N_0$	$\xi_{ij}$
21	-0.884818	0.339440	0.999966
32	0.534001	0.339440	> 1
34	0.534001	-0.232654	> 1
45	-0.945883	-0.232654	0.999989
54	-0.945883	-0.232654	0.999989

normal forces has reduced the collapse load by 8% compared to the simplified solution that takes into account only the bending moments.  $\square$

To emphasize the physical meaning of individual variables, equations and transformations, we have presented the solution of the preceding example in simple terms and in a scalar notation. The reader is advised to think over the structure of the problem, the relation between the scalar and matrix notations, and the relation between the straightforward solution technique used in the example and the simplex method. Problems 13.7 and 13.8 should provide some useful guidelines regarding these considerations.

PROBLEMS

**Problem 13.1:** Construct the elastic and plastic limit envelopes for a) the I-section in Figures 13.18(a),(b) the T-section in Figure 13.18(b).

**Problem 13.2:** Construct the elastic and plastic limit envelopes for an idealized sandwich section (consisting of two thin flanges and a negligible web) and derive the expression for the parameter  $h_0 = M_0/N_0$ .

**Problem 13.3\*:** Prove that the quantity  $c$  evaluated from (13.78) is always positive. Hint: Note that  $c$  is the scalar product of two vectors. Consider their physical meaning, and exploit the properties of the elastic domain.

**Problem 13.4:** Construct a table showing duality of the static and kinematic formulations derived in Section 13.3.

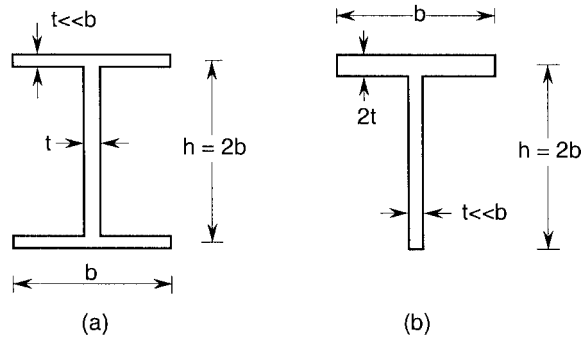


Figure 13.18 Cross-sections for Problem 13.1

Hint: Some equalities will have to be multiplied by  $-1$  to match the signs in the primal and dual problem.

**Problem 13.5:** Show that the simplified kinematic formulation (7.7)–(7.11) can be regarded as a special case of the general kinematic formulation (13.93)–(13.96).

**Problem 13.6\*:** Formulate precisely the conditions under which the simplified theory (neglecting the effect of axial forces) gives an upper bound on the actual safety factor. In other words: in which cases can the presence of normal forces increase the safety factor?

Hint: Note that the simplified condition of plastic admissibility  $|M| \leq M_0$  does not always have to be an exterior approximation of the more exact condition that takes into account interaction with normal forces.

**Problem 13.7:** Present the solution of Example 13.5 in the matrix form. Link equations appearing in the example to the general matrix equations, write matrices  $N$ ,  $S$ ,  $P$ ,  $S^T N$ ,  $P^T N$  and  $P^T N \bar{f}$  explicitly, and show which matrix operations correspond to individual steps of the solution. Construct the kinematic matrix  $B$  and derive matrices  $S$  and  $P$  by Gauss transformations.

**Problem 13.8\*:** It seems that, in Example 13.5, we solved a linear programming problem without applying the simplex technique. Formulate the complete problem (13.101)–(13.104) and show how the solution procedure applied in Example 13.5 relates to the simplex method.